Biomaterials Advances 134 (2022) 112586

Contents lists available at ScienceDirect

Biomaterials Advances

journal homepage: www.elsevier.com/locate/bioadv

In vivo evaluation of oxidized multiwalled-carbon nanotubes-mediated hyperthermia treatment for breast cancer

Muhammad Redza Mohd Radzi [a], Nur Amanina Johari [a], Wan Fatin Amira Wan Mohd Zawawi [a], Nurliyana Ahmad Zawawi [a], Nurriza Ab. Latiff [a,d], Nik Ahmad Nizam Nik Malek [a,b], Asnida Abdul Wahab [c], Maheza Irna Salim [c], Khairunadwa Jemon [a,d,*]

[a] Department of Bioscience, Faculty of Science, Universiti Teknologi Malaysia, 81310 Johor Bahru, Johor, Malaysia
[b] Centre for Sustainable Nanomaterials (CSNano), Ibnu Sina Institute for Scientific and Industrial Research (ISI-ISIR), Universiti Teknologi Malaysia, 81310 Johor Bahru, Johor, Malaysia
[c] School of Biomedical Engineering and Health Sciences, Faculty of Engineering, Universiti Teknologi Malaysia, 81310 Johor Bahru, Johor, Malaysia
[d] Cancer and Infectious Diseases Research Group, Health and Wellness Research Alliance, Universiti Teknologi Malaysia, 81310 Johor Bahru, Johor, Malaysia

ARTICLE INFO

Keywords:
Breast cancer
Carbon nanotubes
Functionalization
Hyperthermia
Near-infrared radiation

ABSTRACT

Breast cancer is one of the most common types of cancer that contribute to high mortality worldwide. Hyperthermia (HT) was introduced as one of the alternative treatments to treat breast cancer but has major drawback of damaging normal adjacent cells. This study explores the integration effect of multiwalled-carbon nanotubes (MWCNTs) in combination with hyperthermia treatment for breast cancer therapy regimes. In this study, acid-functionalized MWCNTs (ox-MWCNTs) were prepared by acid washing methods using H_2SO_4/HNO_3 (98%/68%) with the ratio of 3:1 (*v*/*v*) and characterized by colloidal dispersibility test, FTIR, TGA, XRD, FESEM and EDX analysis. EMT6 tumor-bearing mice were treated with ox-MWCNTs in combination with local HT at 43 °C. The tumor progression was monitored and the influence of immune response was evaluated. Results from this study demonstrated that mice from ox-MWCNTs in combination with local HT treatment group experienced complete tumor eradication, accompanied by a significant increase in median survival of the mice. Histological and immunohistochemical analysis of tumor tissues revealed that tumor treated with combined treatment underwent cell necrosis and there was a significant reduction of proliferating cells when compared to the untreated tumor. This observation is also accompanied with an increase in Hsp70 expression in tumor treated with HT. Flow cytometry analysis of the draining lymph nodes showed an increase in dendritic cells infiltration and maturation in mice treated with combined treatment. In addition, a significant increase of tumor-infiltrated $CD8^+$ and $CD4^+$ T cells along with macrophages and natural killer cells was observed in tumor treated with combined treatment. Altogether, results presented in this study suggested the potential of ox-MWCNTs-mediated HT as an anticancer therapeutic agent, hence might be beneficial in the future of breast cancer treatment.

1. Introduction

Breast cancer is known as one of the most common types of cancers diagnosed among women and the leading cause of death due to cancer in women [1]. In 2020, according to the National Cancer Institute (NIH), breast cancer remained to be the highest type of cancer that occurred worldwide, with the estimated new cases and deaths in the U.S are 276, 480 and 42, 170 deaths, respectively. Despite the advancements in cancer diagnosis and treatments, the increased fatality rate of breast cancer is certainly linked to breast cancer resistance to current conventional therapies [2–5]. Current cancer therapy strategies aimed to introduce minimally invasive protocols with maximum ability to eradicate primary tumor and prevent its recurrence. Such preferences require strategies to localize and enhance high cancer specificity, low toxicity and to avoid the destruction of healthy adjacent cells [6]. In light of that, hyperthermia (HT) has been acknowledged as one of the convincing alternative therapies in cancer treatment. HT which elevates normal body temperature is designed to stimulate and activate the immune system, hence shown potentials in treating the early stage of breast tumor [7–9].

During the treatment, the tumor mass was heated at temperature ranging from 39 °C to 50 °C [10]. Previous studies showed that HT stimulated by near-infrared radiation (NIR) has shown positive outcomes in cancer treatment [11–14]. Practically, HT has been incorporated as an adjunctive therapy that complements other conventional therapies such as surgery, chemotherapy and radiotherapy [15]. Even though HT monotherapy has shown promising effects in breast cancer management, its drawbacks such as low heat retention time and non-uniform heat distribution limit its exploitation. Hence, few improvement strategies have been taken into

* Corresponding author at: Department of Biosciences, Faculty of Science, Universiti Teknologi Malaysia, 81310 Skudai, Johor, Malaysia.
E-mail address: khairun_nadwa@utm.my (K. Jemon).

http://dx.doi.org/10.1016/j.msec.2021.112586
Received 7 July 2021; Received in revised form 1 November 2021; Accepted 28 November 2021
Available online 8 December 2021

consideration, one of them includes the application of nanoparticles as the hyperthermic agent. Various nanoparticles (NPs) have been investigated to enhance the effect of HT, including carbon nanotubes (CNTs) [16], cadmium selenide [17], hydroxyapatite [18] and magnetite nanoparticles (MNPs) [19]. Due to specificity and sensitivity of HT, NPs were modified and tested for their durability, thermal conductivity and systemic toxicity. Among them, CNTs have gained a huge attention due to their potential for simultaneous imaging and therapy, which has been widely reported in biomedical practice involving HT [3,5,16,20]. CNTs may exist in different form, depending on the synthesis protocols. The most commonly available form of CNTs is single-walled carbon nanotubes (SWCNTs) and multi-walled carbon nanotubes (MWCNTs) [21]. CNTs possessed extraordinary physiochemical properties such as low toxicity, stable and most importantly high thermal conductivity which is vital to maintain a longer heat retention time in the tumor microenvironment during the treatment [3,16,22]. While having such beneficial properties, modification of CNTs through acidification or polymerization-based coating can facilitate its biocompatibility and bioavailability inside the body alongside the reduction of systemic toxicity level post-administration [5,23]. Additionally, previous studies found out that CNTs in combination with HT could stimulate both innate and adaptive immune responses as potential anticancer therapy [7,8].

Particularly, studies of both functionalized SWCNTs and MWCNTs with HT have shown promising outcomes in reducing breast tumor especially in the early stage of breast cancer. The study by Jolesch, Elmer [24] and co-workers indicated the induction of heat shock protein 70 (Hsp70) expression in tumors from combined treatment could activate the immune response [13,24,25]. Despite the promising outcomes, what and how oxidized MWCNT (ox-MWCNT) in combination with HT affects the stimulation of immune response, for example, the activation and, infiltration of immune cells requires extended understanding for future application. This study emphasized the effect of the intratumoral route of CNTs administration with local HT therapy in mice-bearing breast tumor. It aims to investigate the effect of ox-MWCNT associated with HT treatment in reducing the EMT6 breast tumor burden *in vivo*.

2. Materials and methods

2.1. Preparation of oxidized MWCNTs and characterization

In this study, ox-MWCNTs were prepared by the acid surface modification method, according to the protocols described in Zawawi et al. [30]. Briefly, pristine MWCNTs (p-MWCNTs) (Timesnano, Chengdu Organics Chemicals Co. Ltd., China) were treated with 400 mL of H_2SO_4/HNO_3 (98%/68%) acid mixture (ν/ν: 3/1). Subsequently, successful preparation of the ox-MWCNTS were confirmed using colloidal dispersion test, Fourier transform infrared (FTIR) spectroscopy, X-ray diffraction (XRD), Thermogravimetric analysis (TGA), Field emission electron microscopy (FESEM) and energy dispersive X-ray (EDX). The dispersibility test of p-MWCNTs and ox-MWCNTs were examined by sonicating them in deionized water following observation at determined time intervals for 20 days. Both p-MWCNTs and ox-MWCNTs were examined using Fourier Transform Infrared (FTIR) spectroscopy at a spectral range of 4000 to 400 cm^{-1} using Perkin Elmer Spectrum One (USA) to observe the spectrum peak of functional groups. The XRD pattern of the MWCNTs were obtained through Rigaku SmartLab X-ray diffractometer (Japan), using high-intensity Cu Kα radiation (λ = 1.54065 Å) from 10° to 90° as the range of 2θ. The TGA analysis was performed using nitrogen gas at 60 mL/min. The TGA analyzer used was DTG-60H (Shimadzu, Japan). Morphological and elemental analyses of MWCNTs were observed using FESEM and EDX analysis equipment of Hitachi UHR FE-SEM SU8020 (Japan).

2.2. In vivo tumor treatment experiment

Female Balb/c mice (8–10 weeks old) were purchased from the Animal Resources Unit (ARU), Universiti Putra Malaysia (UPM), Malaysia. All animal experiments were performed according to protocols approved by Universiti Kebangsaan Malaysia Animal Ethics Committee (UKMAEC), Malaysia (UTM/2019/KHAIRUNADWA/25-SEPT./1045-SEPT.-2019-DEC.-2020). Mice were inoculated with 5 × 105 EMT6 murine breast cancer cells (ATCC, CRL-2755) in 100 μL phosphate buffered-saline (PBS, pH 7.4) into the right flank subcutaneously (s.c.). At day 7 post-inoculation, tumors with the average of 30 mm^2 in size were injected with 50 μL of 2 mg/mL ox-MWCNTs. Then, the tumors were subjected to local HT *via* NIR radiation at 750 nm using water filtered infrared-A wIRA, Hydrosun 750 (Germany) with the power density of 1.5 W/cm^2 at 43 °C for 30 min for mice with local HT treatment and maintained for 10 min for mice combined with ox-MWCNTs. HT treatment was applied three times consecutively for three days. The tumor progression was measured using a digital caliper, and the survival median of the individual mouse was tracked. All mice were sacrificed when the tumor size achieved a maximum allowable size of 150 mm^2.

2.3. Histological analysis

Tumor tissue was harvested 24 h after the third HT treatment and fixed in 10% neutral-buffered formalin and embedded in paraffin for sectioning. Formalin-fixed paraffin-embedded (FFPE) tissue sections (4 μm) were deparaffinized in xylene followed by rehydration with a series of alcohol and propan-1-ol washes. For pathological examinations, tissue sections were subjected to hematoxylin & eosin (H&E) staining and observed using a light microscope (Nikon, Japan).

2.4. Immunohistochemical analysis

Formalin-fixed paraffin-embedded (FFPE) tissue sections were deparaffinized in xylene and rehydrated with a series of alcohol washes. Antigen was retrieved using sodium citrate (pH 6) and the sections were blocked with 5% skim milk for 30 min. The deparaffinized sections were incubated with primary antibody anti-mouse PCNA (clone c19, Abcam) or anti-Hsp70 (W27, Santa Cruz Biotechnology) overnight at 4 °C. After washing, the sections were further incubated with a secondary antibody, Alexa Fluor 488 goat anti-mouse IgG and counterstained with DAPI after 30 min. Sections were then mounted with SlowFade Diamond (Thermo Fisher, USA) incubated overnight at 4 °C. All slides were observed using a fluorescence microscope and the positively stained cells were quantified by ImageJ software (https://imagej.nih.gov/ij/).

2.5. Preparation of lymphocytes and tumor cells for flow cytometry

Inguinal and axillary lymph nodes were harvested 10 days post-inoculation. Single cells that were released from the tissue were filtered through a 70 μm cell strainer and centrifuged at 400 ×*g* for 5 min. Meanwhile, tumor tissues were harvested 21 days post-inoculation and incubated with non-enzymatic dissociation buffer (NEDB) and tumor digestion medium for 30 min at room temperature. Then, tumor cells were filtered through a 70 μm cell strainer and centrifuged at 400 ×*g* for 5 min before being treated with erythrocyte lysis buffer for 5 min at room temperature. The cells were filtered through a new 70 μm cell strainer and centrifuged at 400 ×*g* for 5 min. Both lymphocytes and tumor cells were washed and resuspended at 1 × 10^7 cells/ml in FACS buffer. Cells were incubated with Alexa Fluor 488 (AF488)-conjugated anti-CD11c (Biolegend, CA, USA), PE-conjugated anti-CD80, APC-conjugated anti-CD86, APC-conjugated anti-MHC-I, APC/Cy7-conjugated anti-MHC-II, AF488-conjugated anti-CD4, APC-conjugated anti-CD3, PE-conjugated anti-CD45, PE/Cy7-conjugated anti-CD25, AF647-conjugated anti-FoxP3, FITC-conjugated anti-CD49b, APC-conjugated anti-CD11b, AF488-conjugated anti-Gr-1, and AF488-conjugated anti-CD8 antibodies (BD Biosciences, CA, USA), washed again and fixed with fixation medium (Fix & Perm Kit, Invitrogen).

The cells were then washed and resuspended in FACS buffer (1% BSA and 0.1% sodium azide in PBS).

2.6. Flow cytometric analysis

Samples were acquired using BD FACSVerse cytometer (Becton Dickinson, CA, USA). Lymphocytes and tumor cells were identified based on their forward scatter (FSC) and side scatter (SSC) properties. Unlabeled cells and labeled cells were used to adjusts the channel voltages and compensate for the spectral overlap between fluorochromes used. In the experiments, BD Comp Beads compensation particles set (BD Bioscience) were used to optimize the fluorescence compensation settings. Data were analyzed using Flow-Jo software version 10.6.1 (Tree Star, OR, USA).

2.7. Statistical analysis

The normal distribution of the data was assessed by the Shapiro-Wilk test. Comparisons in survival between experimental groups were analyzed using Mantel-Cox analysis while the comparisons between experimental groups were determined by either Student's *t*-test or Mann Whitney *U* test. All statistical analysis was carried out within Prism version 7.0 (GraphPad Software, CA, USA).

3. Results

3.1. Characterization of ox-MWCNTs

Validation of ox-MWCNTs modification was performed by several physicochemical and thermal characterization analyses. Colloidal dispersibility was performed as shown in Fig. 1A, where this analysis produced a quick-qualitative observation to monitor the dispersibility of MWCNTs in the aqueous environment. ox-MWCNTs showed a stable dispersion even until 20 days post-sonication while p-MWCNTs showed low dispersion in deionized water and began to sediment after 30 min.

Further confirmation was done by performing FTIR spectroscopic analysis as shown in Fig. 1B. Strong peaks at 3550–3200 cm^{-1} and 1225–1200 cm^{-1} indicates the presence of functional groups OH and CO respectively, in ox-MWCNTs. On the other hand, p-MWCNTs also showed a weak and broad-peak at 3400 cm^{-1} which represent the OH group on the surface of MWCNTs. Besides, the XRD data provides the preserved amorphous structure of both MWCNTs. As shown in Fig. 1C, ox-MWCNTs displayed a slight increased in intensity at 25° of the 2θ plane but non-significant enough as compared to p-MWCNTs. As shown in the TGA spectra of the samples (Fig. 1D), both MWCNTs tested experienced weight loss due to temperature-dependent decomposition rate. It was observed that ox-MWCNTs suffered 6% weight loss while p-MWCNTs experienced 3%

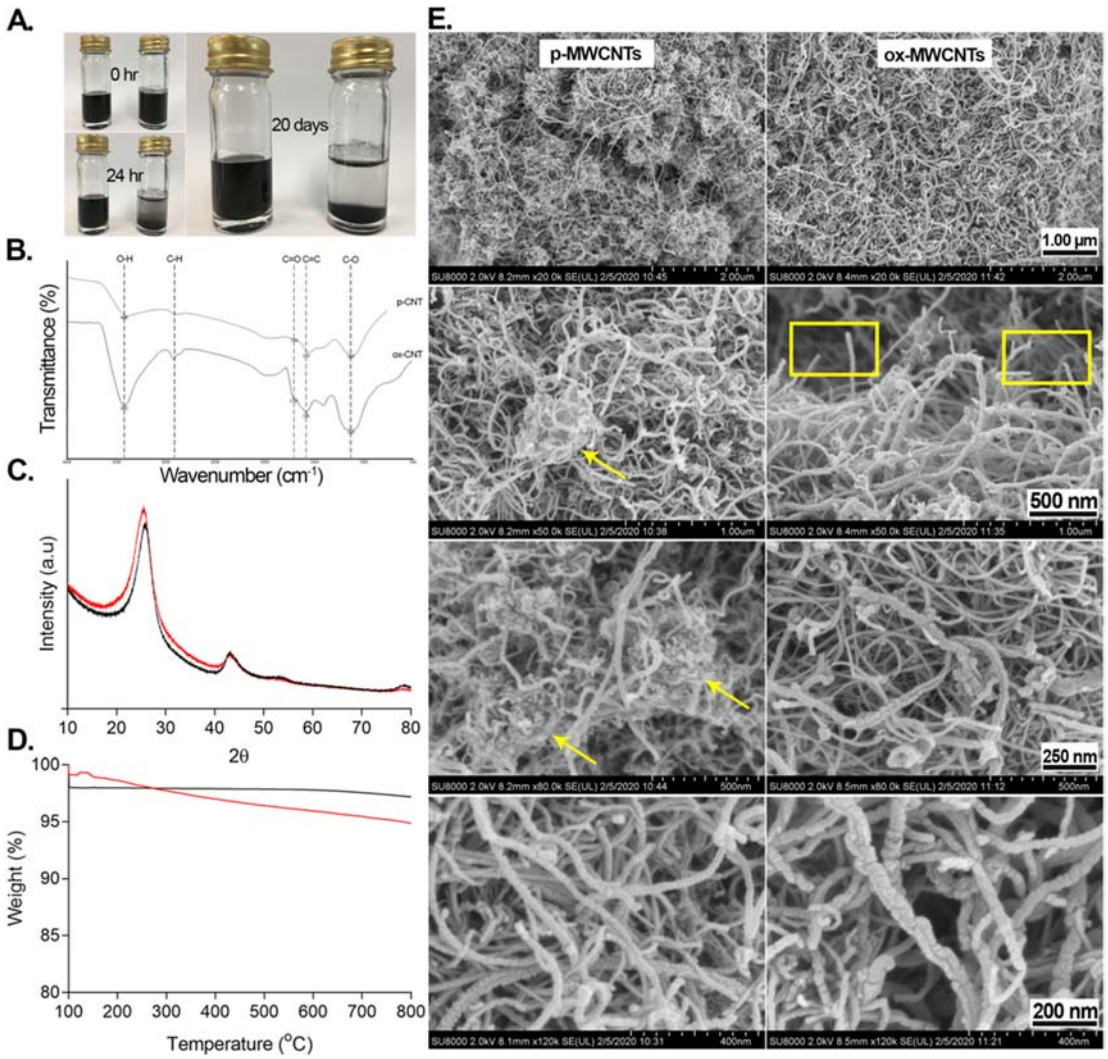

Fig. 1. Characterization analysis profiles of p-MWCNTs and ox-MWCNTs. (A) Colloidal dispersibility test in deionized water. *Right*: ox-MWCNTs. *Left*: p-MWCNTs (B) FTIR spectrum of MWCNTs. (C) XRD patterns of MWCNTs. *Red*: ox-MWCNTs. *Black*: p-MWCNTs. (D) TGA curves of MWCNTs. *Red*: ox-MWCNTs. *Black*: p-MWCNTs. (E) FESEM images of MWCNTs.

weight loss after being combusted to 800 °C. After all, both MWCNTs displayed high thermal stability which suggested their suitability for hyperthermia therapy.

On the other hand, the FESEM images indicated the physical visualization of ox-MWCNTs after the acid washing process. Fig. 1E depicts the comparison of p-MWCNTs and ox-MWCNTs outer structures. ox-MWCNTs have shown the ruptured morphology with the cut effect at their ends alongside the groovy or twisted surface (indicated with yellow boxes). ox-MWCNTs are observed to possess a rougher and shortened tubular length as compared to p-MWCNTs. Meanwhile, p-MWCNTs exhibited a fluffy, long tubular morphology with several clumps (yellow arrow; Fig. 1E). In addition, p-MWCNTs have been observed to have a smoother surface compared to ox-MWCNTs. Studies on the EDX analysis further supported other characterization analyses on the validation of MWCNTs modification. As shown in Table 1, all the elemental compositions that existed on the MWCNTs were identified. The most abundant elements composition embedded in MWCNTs were carbon and oxygen. As expected, ox-MWCNTs showed an increment up to 19.31% in the amount of oxygen after being introduced to surface modification. In contrast, the carbon composition inside ox-MWCNTs was significantly reduced to 63.57% as compared to p-MWCNTs. Altogether, these characterization analyses validated the modification of ox-MWCNTs *via* acid surface modification prior to application *in vivo*.

3.2. ox-MWCNTs-mediated hyperthermia completely eradicates tumor in tumor-bearing mice

This study firstly evaluated the therapeutic anticancer effect of ox-MWCNTs-mediated HT in eliminating EMT6 breast tumor. Mice were inoculated with EMT6 cells and tumor-bearing mice were then subjected to either treatment with HT monotherapy, ox-MWCNTs only or combination of HT and ox-MWCNTs (hereafter; combined). Untreated tumor-bearing mice serve as the control group. Tumor growth was monitored to determine the treatment efficacy (Fig. 2A). Fig. 2B-E depicts the tumor growth of individual mice according to each treatment group. Results demonstrated that HT-treated mice displayed a reduction in tumor size in three out of the six mice (50%), with a complete tumor disappearance within two weeks post-treatment. Interestingly, a 100% (seven out of seven) complete tumor eradication was observed in mice treated with combined treatment within 40 days post-treatment. This was accompanied by greater mice survival benefit ($P < 0.01$; Mantel-Cox analysis) seen in the combined group as compared to HT, ox-MWCNTs and untreated group, with a median survival of 50, 38.5, 25 and 21.5 days, respectively (Fig. 2F). These results also indicate that the untreated and ox-MWCNTs-treated group suffered a 0% survival rate, HT-treated group with 50% survival rate, meanwhile combined group achieved 100% survival rate.

3.3. ox-MWCNTs-mediated HT promotes tumor necrosis, reduces cancer cells proliferation and upregulates Hsp70 expression

To understand the effect of ox-MWCNTs in combination with HT treatment on tissue, tumors were harvested 24 h post-treatment, fixed and stained with H&E for histological evaluation (Fig. 3A). As shown in Fig. 3B, both untreated and ox-MWCNTs-treated tumor tissues exhibited normal cell morphology with the presence of intact cells with large nuclei and well-maintained cytoplasm. In contrast, tumor treated with HT experienced loss of normal cell architecture with nuclei shrinkage, along with the formation of pale eosinophilic cytoplasm and reduced purple viable nuclei. These results are however more prominent in tumor treated with ox-MWCNTs in combination with HT treatment, where almost no viable cells were observed, suggesting the addition of ox-MWCNTs in HT treatment could aggressively induced tumor necrosis.

To support this, the cells proliferating activity was evaluated by staining the tumor tissue sections with anti-PCNA antibody (Fig. 3C). Proliferating Cell Nuclear Antigen (PCNA) is essential for cells replication and is typically used as a marker for cell proliferation. Images from all groups of treatments were retrieved and quantitative analysis of positive anti-PCNA stained cells was performed corresponding to the proliferative index of tumor cells as displayed. Results demonstrated a large number of actively proliferating cells in both untreated and ox-MWCNTs-treated tumor. In contrast, HT-treated tumor showed a significant reduction ($P < 0.01$; Student's *t*-test) of PCNA-positive cells. However, a greater reduction ($P < 0.005$; Student's *t*-test) was observed in tumor treated with ox-MWCNTs and HT combination (Fig. 3E), suggesting that this treatment benefited in arresting cell proliferation.

HT has been widely reported to induce heat stress in the tumor microenvironment thus normally caused an increase in the expression of heat shock protein. Theoretically, the induction of heat by NIR radiation used in this study will stimulate the expression of Hsp70 in the tumor microenvironment either with the administration of ox-MWCNTs or HT alone. Therefore, the expression of Hsp70 following treatment was investigated. The tumor tissues were stained with an anti-Hsp70 antibody as outlined in Fig. 3A. Fig. 3D demonstrates negative staining of Hsp70 in the untreated tumor. Likewise, there was no Hsp70 expression detected in the ox-MWCNTs-treated tumor. In contrast, Hsp70 was abundantly expressed in the tumor of both HT-treated and combined treated mice. This result reflects the stress response induced by NIR radiation, which might play an important key role in tumor microenvironment immunomodulatory effects.

3.4. ox-MWCNTs-mediated HT increases DCs maturation in the draining lymph nodes

It has been previously reported that Hsp70 expression may lead to upregulation of immunomodulatory effects. To understand the immune response following ox-MWCNTs and HT combined treatment on established solid tumors, we observed dendritic cells (DCs) maturation in the draining lymph nodes (dLN). In this study, mice were sacrificed 10 days post-inoculation and lymphocytes isolated from the dLN were stained with anti-CD11c antibody, a specific marker of DCs, together with their maturation markers, anti-MHC-I, anti-MHC-II, anti-CD80 and anti-CD86 antibodies (Fig. 4A). The lymphocytes population was gated based on the forward scatter (FSC) and side scatter (SSC) profiles and the DCs population was identified as $CD11c^+$ cells (Fig. 4B). As shown in Fig. 4C, it was observed that there was a non-significant increase in the percentage of $CD11c^+$ cells ($P > 0.05$, Student's *t*-test) in mice treated with ox-MWCNTs and HT combined treatment as compared to the untreated group.

The $CD11c^+$ DCs were further analyzed to investigate if the combination of ox-MWCNTs and HT treatment could promote DCs maturation. As shown in Fig. 4D & F, mice treated with combined treatment exhibited a significant increase of MHC-I and CD80 expression ($P < 0.05$; Mann-Whitney *U* test) as compared to untreated. In addition, a non-significant increase of MHC-II and CD86 expression were also observed (Fig. 4E & G). This implies that combined treatment could induce DCs maturation in the dLN as compared to ox-MWCNTs or HT alone treatment, thus suggesting the initiation of immune response affected by the heat stimulation.

Table 1
Elemental composition of p-MWCNTs and ox-MWCNTs from EDX analysis.

Elements	Weight (%)	
	p-MWCNTs	ox-MWCNTs
Carbon	91.2	69.4
Oxygen	6.3	17.0
Molybdenum	0.2	3.7
Cobalt	0.2	2.1
Magnesium	–	7.8
Silica	–	0.1

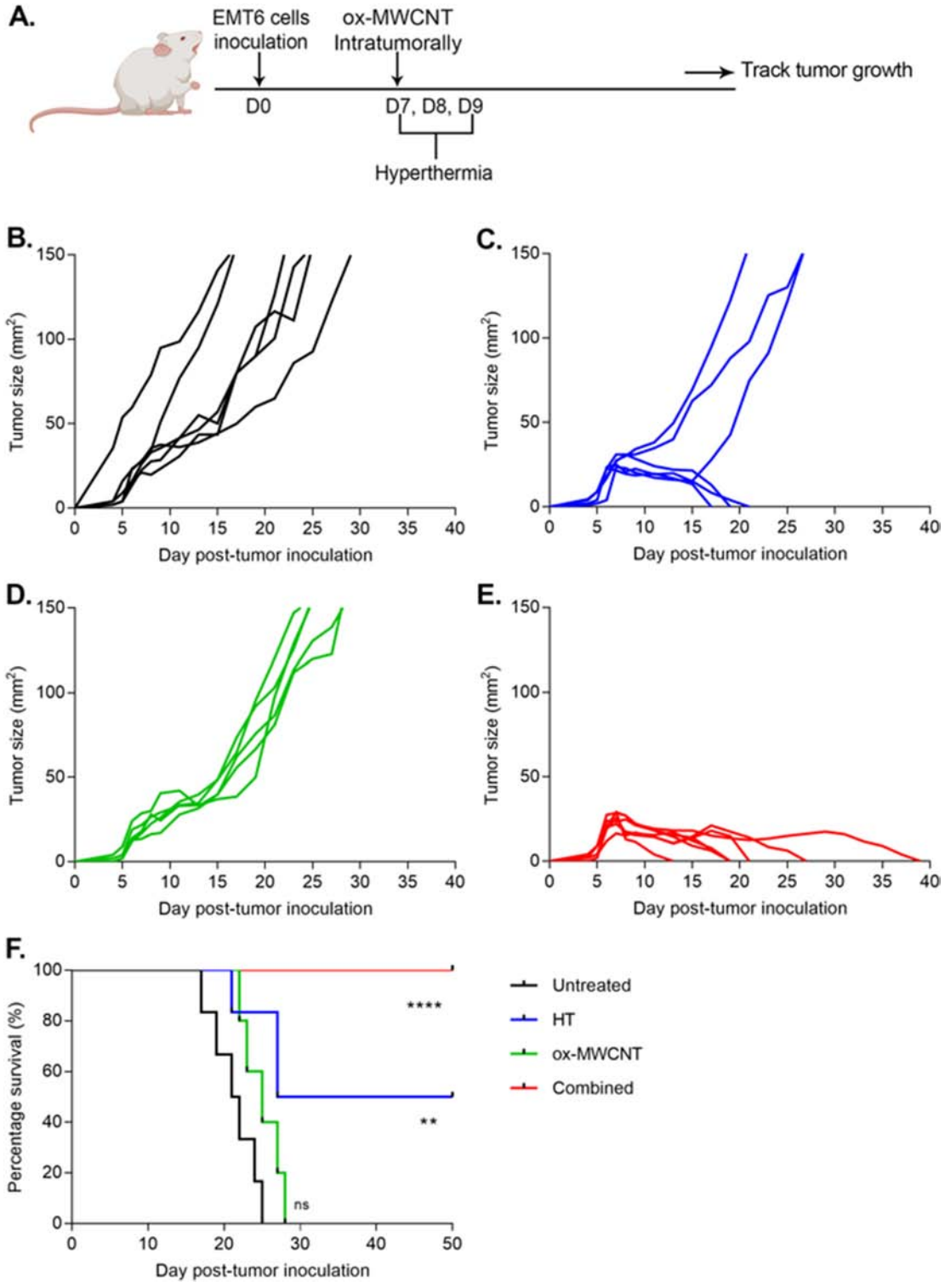

Fig. 2. Combination of ox-MWCNTs and HT treatment eradicates EMT6 tumor. (A) Schematic time course to study tumor progression following treatment. Line graph depicting individual tumor in untreated mice (B), HT (C), ox-MWCNTs (D) and combination of ox-MWCNTs and HT (E) treated group. F) Survival curve of mice from all group of treatment within 50 days of treatment (F). $n = 5$–7 mice per group. $^{****}P < 0.001$, $^{**}P < 0.01$, *ns*, non-significant (Mantel-Cox test).

3.5. ox-MWCNTs-mediated HT increases the infiltration of T cells and decreases Tregs population in breast tumor

The increased in DCs maturation has led us to further investigate whether these effects on DCs may influence the recruitment of adaptive immune cells into the tumor tissue, which may subsequently suppress the tumor progression. As outlined in Fig. 5A, tumors were harvested and stained for respective T cells marker. The populations of T lymphocytes were either gated based on the expression of CD3 and CD8 surface markers (CD8 cytotoxic T cells) or CD3 and CD4 surface markers (CD4 helper T cells) (Fig. 5B). Results showed that HT treatment significantly increase ($P < 0.05$; Student's *t*-test) the infiltration of $CD3^+CD4^+$ and $CD3^+CD8^+$ T cells, into the tumor as compared to the untreated group. However, further increment was observed in mice from combined

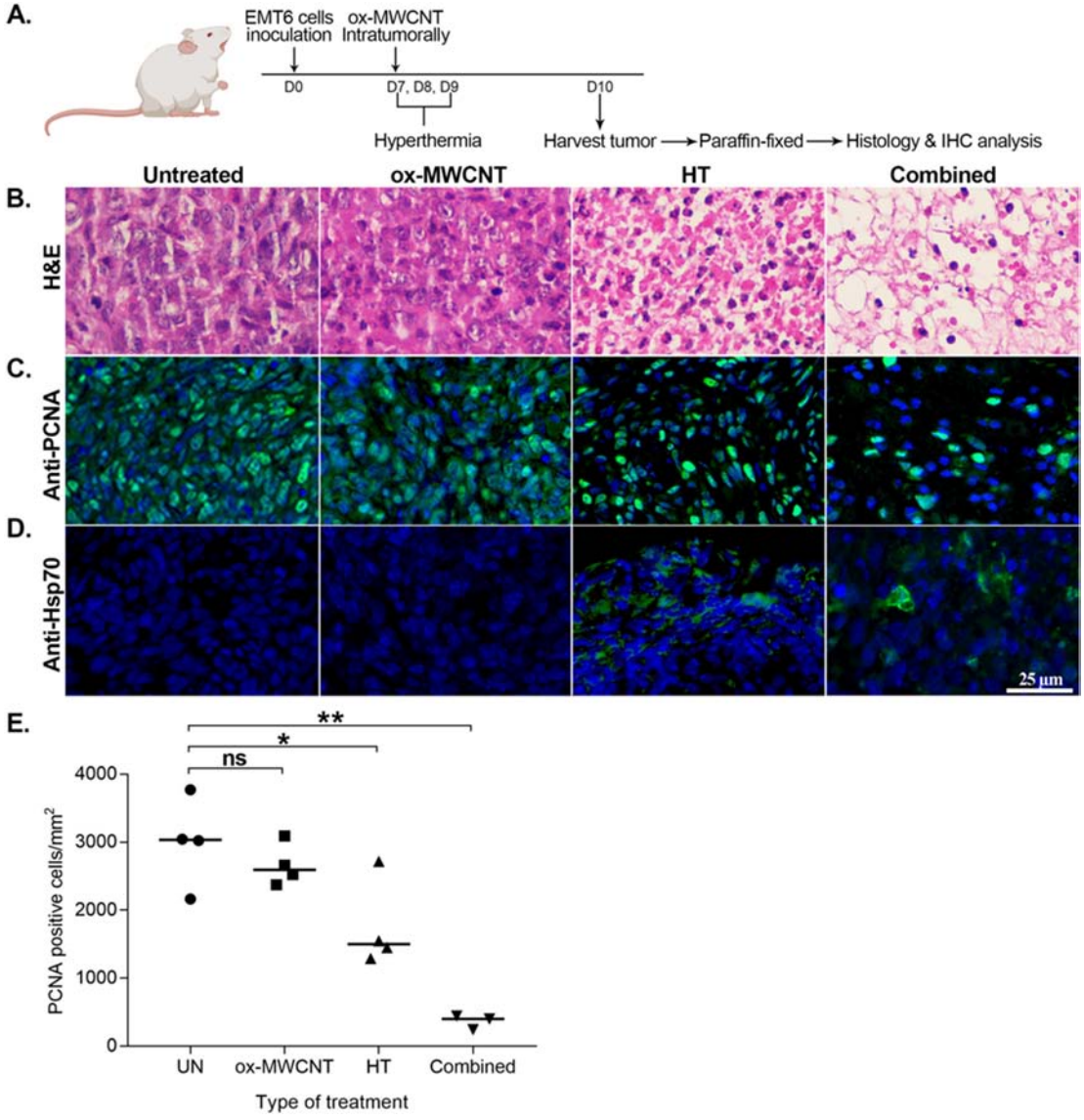

Fig. 3. Representatives images of histological and immunohistochemical analysis of tumor tissues. (A) Schematic time course to examine pathological changes in tissue. Histological images of H&E stained tissue (B). Fluorescence micrographs showing the expression of PCNA (C) and Hsp70 (D). Scale: 25 μm. Magnification: 40×. (E) Graph showing PCNA positive-stained cells per mm^2. $n = 3$–4 mice per group. $^{**}P < 0.01$, $^{*}P < 0.05$, *ns*, non-significant (*t*-Test).

treatment, indicating effective infiltration of cytotoxic and helper T cells within the tumor microenvironment following ox-MWCNTs and HT combined treatment (Fig. 5C-D).

We next evaluated the effect of combined treatment on the infiltration of regulatory T cells (Tregs). Tregs are a subpopulation of $CD4^+$ T cells, described as co-expressing CD25 and Foxp3 markers. As shown in Fig. 5E, combined-treated mice induced a significant reduction ($P < 0.05$; Student's *t*-test) of tumor infiltrated Tregs, as compared to the untreated group. Meanwhile, tumor treated with monotherapy of HT or ox-MWCNTs showed a slightly higher Tregs percentage as compared to combined treatment, suggesting an effective dampening of the immunosuppressive environment following ox-MWCNTs and HT combined treatment.

3.6. ox-MWCNTs-mediated HT increases the infiltration of NK cells and macrophages in tumor

The initiation of an immune response against tumor cells did not necessarily depend on T lymphocytes activation. It was suggested that innate immune cells such as natural killer (NK) cells and macrophages also contributed to an effective anti-tumor response. Therefore, in this study, we wish to investigate whether combined treatment would affect the infiltration of innate immune cells, particularly NK cells and macrophages at the tumor site. Similarly, tumors were harvested 21 days post-inoculation and subjected to flow cytometric analysis as depicted in Fig. 6A. NK cells were identified as $CD3^-$ $CD49b^+$ cells while macrophages were identified as $CD11b^+$ $Gr\text{-}1^{low}$ cells gated on $CD45^+$ cells (leukocytes) (Fig. 6B). Based on Fig. 6C, combined treatment exhibited a higher percentage of NK cells ($P < 0.05$; Student's *t*-test), as compared to ox-MWCNTs-treated and untreated group which were barely distinguishable. Although HT-treated mice also demonstrated higher NK cells as compared to untreated mice, the combined treatment surpassed this percentage at almost two-fold, suggesting an enhanced NK cells activity following combined treatment. On the other hand, the combined treatment also displayed a significant increase percentage of macrophages ($P < 0.05$; Student's *t*-test), as compared to the untreated group. Along with the observation that macrophages induced by combined treatment were higher than the monotherapy of HT and ox-MWCNTs, these results reflected the synergistic effects of ox-MWCNTs and HT in inducing the infiltration of NK cells and macrophages into the tumor microenvironment. Taken together, findings in this study

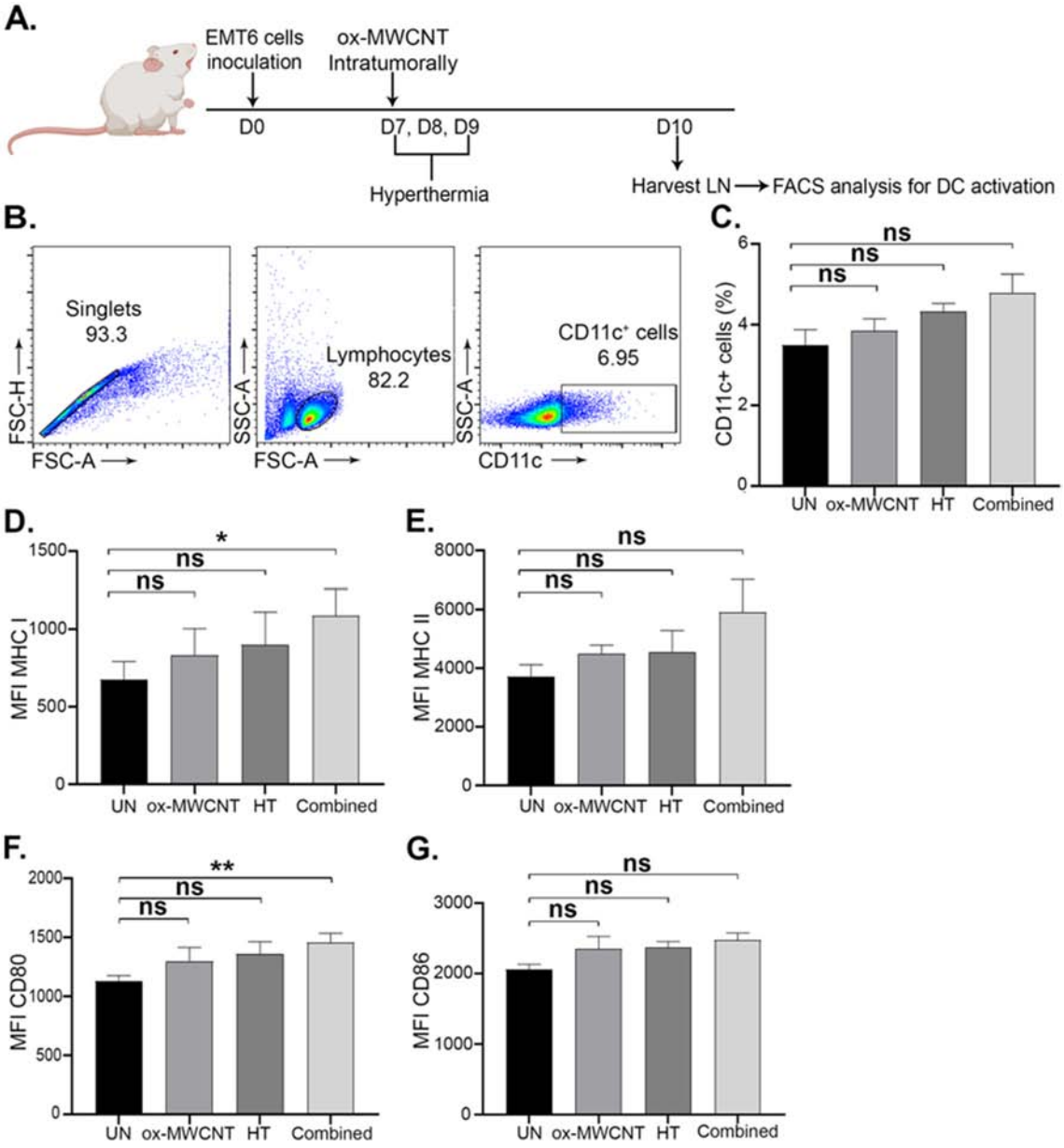

Fig. 4. The effect of combination of ox-MWCNTs and HT on DCs maturation analyzed by flow cytometry. (A) A schematic diagram to depict experimental timeline. (B) Representative dot plots are shown for gating strategy for CD11c dendritic cells in the LN. (C) The percentage (mean ± SEM) of $CD11c^+$ dendritic cells. The geometric MFI (mean ± SEM) for MHC-I (D), MHC-II (E), CD80 (F), and CD86 (G) is shown for each treatment group. $n = 4$–6 mice per group. $^*P < 0.05$, ns, non-significant (Mann Whitney *U* test).

speculate the involvement of both innate and adaptive immune responses in breast tumor eradication.

4. Discussion

Available conventional treatments such as chemotherapy, radiotherapy, and surgery frequently encountered cancer recurrence, poor therapeutic targets, the rise of multidrug resistance tumor and systemic toxicity [2,4,5]. For the past decades, demands on non-conventional treatments for cancers have led to extensive studies worldwide [26]. Due to this, nanomaterials including CNTs have been acknowledged due to their unique properties [27]. We further investigated the therapeutic activity of modified ox-MWCNTs in combination with localized HT treatment as an alternative treatment for breast cancer.

In addition to their stable biochemical characteristics [3,4], MWCNTs possessed valuable physiochemical properties that make them suitable for application in nanotechnology-mediated heat therapy. However, unmodified or pristine MWCNTs are inert, insoluble and low dispersibility thus could cause the aggregation of MWCNTs in blood vessels [28]. Exposure to p-MWCNTs has been associated with inflammation of the respiratory system and lung cancer [29] hence, are not applicable for biomedical purpose. It was reported that the elevation of the hydroxyl and carboxyl groups, attached at the surface of MWCNTs after oxidation can increase their solubility and dispersibility in the polar molecule [28,30]. Therefore, modification of MWCNTs through a series of acid oxidation procedures is required to increase their bioavailability inside tumor microenvironment simultaneously minimizing the toxicity effect of CNTs [4,31]. In this study, results from the dispersibility test indicated that ox-MWCNTs displayed higher dispersibility compared to p-MWCNTs in polar solutions. One of the factors that might contribute to the unstable dispersibility of p-MWCNTs was the hydrophobicity of graphene sidewalls that contribute to strong hydrophobic interaction thus easily aggregated and sedimented in a short period

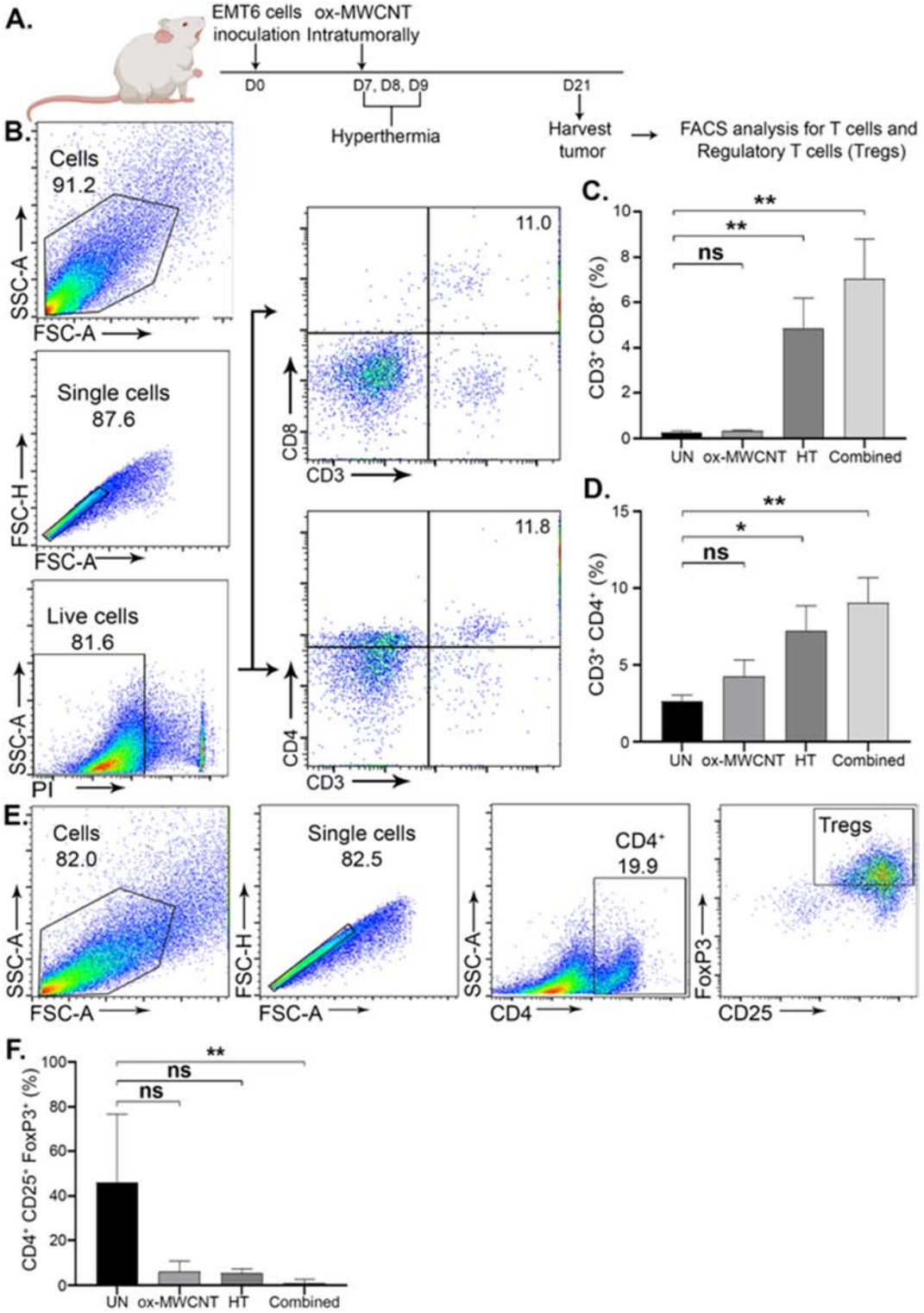

Fig. 5. Combination of ox-MWCNTs and HT increases T cells population while depletes Tregs infiltration in the tumor. (A) Schematic diagram to depict experimental timeline. (B) Representative dot plots are shown for gating strategy for $CD3^+$ $CD8^+$ and $CD3^+$ $CD4^+$ lymphocytes in the tumor. The percentage (mean ± SEM) for $CD3^+$ $CD8^+$ (C) and $CD3^+$ $CD4^+$ (D) is shown. *ns*; non-significant, $^*P < 0.05$, $^{**}P < 0.005$ (Student's *t*-test). E) Representative dot plots are shown for gating strategy for $CD4^+$ $CD25^+$ $FoxP3^+$ regulatory T cells in the tumor. The percentage (mean ± SEM) for $CD4^+$ $CD25^+$ $FoxP3^+$ (F) is shown for each treatment group. $n = 4$–6 mice per group. *ns*; non-significant, $^{**}P < 0.005$ (Mann-Whitney *U* test).

post-dispersion [32]. This evidence was supported by the FTIR spectrum analysis which showed that ox-MWCNTs contain more available hydroxyl and carboxyl groups. The added functional groups provide positively or negatively charge on the surface thus keeping ox-MWCNTs dispersed due to better repulsion from the equally charged particles [30,33]. Meanwhile, the XRD analysis data revealed that the structure of ox-MWCNTs was preserved even after surface modification. The reflection plane (002) is the same for both MWCNTs where diffraction peak at 25° were detected. The XRD patterns indicated the formation of loosely ox-MWCNTs floss [34]. On the other hand, the TGA data suggested that MWCNTs experienced a

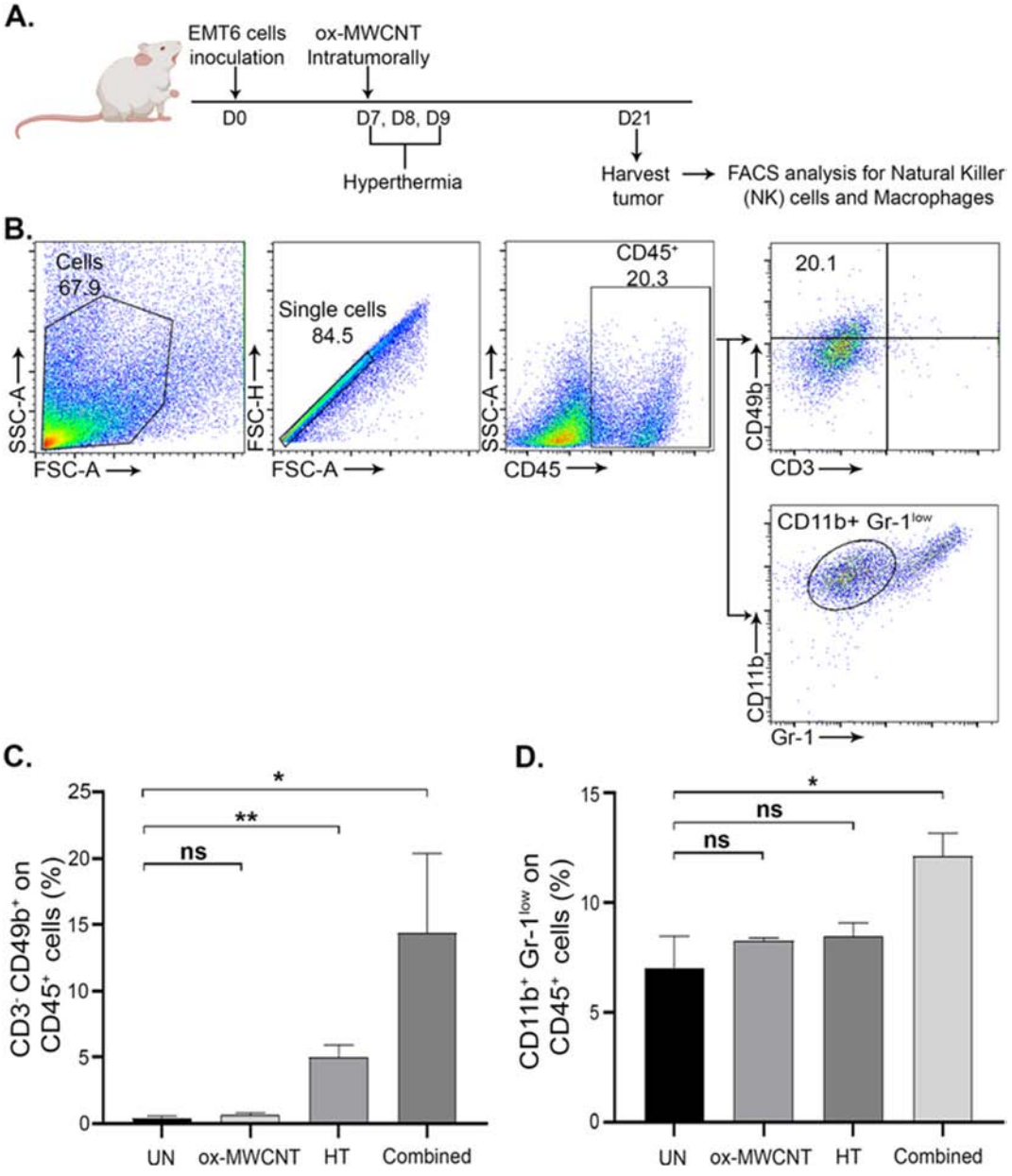

Fig. 6. Percentages of NK cells and macrophages in the tumor tested by flow cytometric analysis after treated with ox-MWCNTs and HT. A) A schematic diagram to depict experimental timeline. (B) Representative dot plots are shown for gating strategy for $CD45^+$ $CD3^-$ $CD49b^+$ natural killer cells and $CD45^+$ $CD11b^+$ $Gr\text{-}1^{low}$ macrophages in the tumor. The percentage (mean ± SEM) for $CD45^+$ $CD3^-$ $CD49b^+$ (C) and $CD45^+$ $CD11b^+$ $Gr\text{-}1^{low}$ macrophages (D) is shown for each treatment group. n = 4–6 mice per group. *ns*; non-significant, $^*P < 0.05$, $^{**}P < 0.005$ (Student's *t*-test).

multistage process of thermal degradation in which the graphene MWCNTs started to oxidize at higher temperature. Other study revealed that MWCNTs started to lose weight due to the combustion at the temperature range of 700 °C–800 °C [35]. p-MWCNTs showed slight thermal degradation while ox-MWCNTs lose more weight. This phenomenon indicates the existence of oxygenated-functional group thus increasing high thermal combustion from the oxidation process. The FESEM images of ox-MWCNTs depicted the formation of a ruptured structure with a groovy surface that allows the decoration of functional groups during the acid washing process [30,34,36]. In contrast, clumps formation in p-MWCNTs portrayed the high content of amorphous carbon as detected in EDX analysis with the stable undisturbed long tube while there was a reduction in carbon content in ox-MWCNTs [37]. From this analysis, it can be concluded that ox-MWCNTs were successfully modified and may function as an excellent hyperthermic agent.

It has been well established that HT exerts anticancer activity either through direct effect by killing off cancer cells or indirect effect by stimulating the immune system inside the patient's body [7,14,24]. In this study, we performed local HT treatment by applying NIR radiation to produce the hyperthermic effect. It has been previously reported that NIR radiation showed promising outcomes in heating specific parts of the tumor thus could avoid the disruption or killing of healthy adjacent cells [7,11,14]. Further improvement has been made in this study where ox-MWCNTs were administered to amplify the effectiveness of HT by providing longer heat retention time, more specific heat distribution and their ability to stimulate the immune system through activation of DCs. Our findings on the progression of tumor growth indicated that combined treatment promoted tumor suppression thus prolonged the life span of the mice. On the same token, histological analysis demonstrated higher necrotic tumor cells in combined-treated tumors as the effect of direct killing of cancer cells.

Besides, combined therapy has demonstrated an increase in tumor suppression activity and also lethal thermal injury that contributed to tumor necrosis [38]. Results on the histology analysis were significant with the results observed through the proliferative cells activity analysis. PCNA, which is a proliferation marker, was commonly identified in breast cancer. This marker was expressed during nucleic acid metabolism which plays a role in DNA replication, DNA excision repair, cell cycle control, chromatin assembly, and RNA replication. Our results showed that combined treatment significantly reduced the cells' proliferation activity which corresponded to the histology analysis earlier. This indicated that the cell cycle of tumor cells was arrested thus no proliferation activity happened within the tumor microenvironment. On top of that, these results supported the evidence on combined treatment efficacy in reducing the rate of cell proliferation thus resulting in the inhibition of breast cancer cells. In contrast, untreated and ox-MWCNTs treated mice highly expressed proliferation marker thus indicating their highly proliferating activity which corresponded to our histology analysis.

Interestingly, HT did not only kill breast cancer cells through lethal thermal injury but also an immune-stimulating mechanism. The stimulation of immune system can be achieved *via* the presentation of foreign particulates or specialized peptides for antibody recognition. In our study, we expected the role of Hsp70 as peptide recognition for antigen presentation. Hsp70 is one of the molecular chaperones that play a key role in immunogenic peptides presentation in cancer immunotherapeutic [24,39]. It is believed that Hsp70 modulated antigen cross-presentation from DCs to $CD8^+$ T cells due to specific antigen recognition from tumor-expressing Hsp70 [25]. Our findings revealed that Hsp70 only being expressed under the heat-inducing environment thus facilitated the stimulation of immune response. HT and combined-treated mice from our study visualized the positive signal of anti-Hsp70 fluorescence staining which indicated the expression of Hsp70 post-heat induction in breast tumor. In correspond to DCs recognition during Hsp70 upregulation, naïve DCs undergone maturation and cross-presented the Hsp70 peptide to inactivated T cells [13]. Hence, mature and activated T cells especially cytotoxic T cells will perform the killing mechanism towards specific breast tumor cells.

DCs are one of the well-known APCs that play critical roles in connecting the innate and adaptive immune system especially as central regulators of the adaptive immune response, and necessary for T cell-mediated cancer immunity. Naïve DCs are known to mature and migrate to the LN after encounter antigens, where they will present the antigens to naïve T cells. It is reported that combined treatment induced DCs migration by upregulating homing receptor CCR7 that mediates DCs migration to the lymph nodes [40]. In addition, released Hsp70 after heat shock is also suggested to stimulate DCs migration for better immunogenicity of tumors [41]. Our results indicated that the combination of HT and ox-MWCNTs treatment may influence the DCs migration at the nearest dLNs, especially the axillary and inguinal LNs. T cell activation by DCs is dependent on the surface expression of MHC-I, MHC-II, and co-stimulatory molecules, CD80 and CD86. Findings from this study revealed that combined treatment can cause DCs maturation and thus further activate both innate and adaptive immune response post-treatment [42,43]. In addition, the combination of ox-MWCNTs and HT treatment showed an even stronger immune stimulation effect if compared with either ox-MWCNTs alone or HT alone. Meanwhile, *in situ* tumor destruction by local HT, may provide a source of antigen for the immune system to induce unique antitumor immunity, as more tumor antigens such as extracellular Hsp70 were released in the tumor microenvironment. Another factor that promotes the upregulation of DCs in combined treatment is that ox-MWCNTs can also induce an adjuvant effect and thus amplify immunostimulatory signals following hyperthermia treatment [44]. After interaction of DCs with ox-MWCNTs and tumor antigen, more immature DCs would be stimulated and migrated to nearby dLNs, undergone maturation which leads to activation of T lymphocytes and then regulate subsequent immunities.

The upregulation of infiltrated T cells response in combined treatment might be due to several mechanisms. This includes the increase in the frequency of DCs into the LNs, increased expression of MHC-I, MHC-II, and co-stimulatory molecules, CD80 and CD86 as well as upregulation of chemokines and cytokines. As one of the APCs, DCs play a crucial role in antigen cross-presentation on T cells in the LNs and consequently activating them. The upregulation in the T cells response in combined treatment observed in the study could be related to an increase of the DCs frequency and therefore increasing their immunosurveillance. During HT treatment, heated tumor cells released Hsp70 on the cells' surface which was taken up and processed by the DCs. The Hsp70 is then presented on MHC-I and MHC-II and recognized by T cells, resulting in the activation of the immune response. It has been shown in a previous study that DCs maturation markers increased in the HT-treated tumors and thus improve the T cells activation and migration to the tumors. The upregulation effects mediated by the combined treatment have created a favorable environment for anti-tumor responses. In addition, similar results were found where the combined treatment reduced Tregs and increase $CD4^+$ and $CD8^+$ T cells infiltration which improved the effective anti-tumor responses on tumor cells [42]. In contrast, downregulation of Tregs in the combined treatment suggested that this treatment could prevent *in situ* immunosuppression. This situation provides a favorable condition for effective cytotoxic killing activity of $CD8^+$ T cells, owing to the suppression of Tregs [45]. Since Tregs has known to counter back the immunomodulatory effects of other immune cells, their downregulation could be beneficial in avoiding tumor survivability post-treatment. These results indicated that the local HT and ox-MWCNTs strategy can amplify anti-tumor responses and stimulate the immune responses for effective T cells mediated responses thus providing a potential option for breast cancer therapy.

The expression of Hsp70 has also been shown to induce chemotaxis and capacity of NK cells by making the tumors more susceptible to recognition by NK cells. Therefore, the present study has demonstrated that a combination of HT and ox-MWCNTs can significantly increase the anti-tumor activity of NK cells. This study explored the influence of ox-MWCNTs on the macrophages in the tumor following HT treatment. Macrophages upregulation indicates that CNTs can increase tumor toxicity in conjunction with HT due to the properties of the photothermal transducer [27]. It is reported that the combination of ox-MWCNTs and HT reaction decreased the tumor burden and at the same time revealed tumor antigens such as Hsp70 which stimulate the recruitment and phagocytosis responses of macrophages together with ox-MWCNTs. Hence, this study demonstrates the synergistic relationship of ox-MWCNTs between HT and immunological stimulation, which increases the cytotoxicity and immunogenicity of tumor cells, leading to increased destruction of tumor cells and anti-tumor response.

Hence, the possible anti-tumor immune response induced by the combination of ox-MWCNTs and HT treatment in solid EMT6 tumor was proposed in Fig. 7. In this study, the combination of ox-MWCNTs and HT appeared to affect both innate and adaptive immune responses more effectively than HT treatment alone. The elevated temperature induced by the treatment induced expression of Hsp70 at a higher level in tumor microenvironment. This elevated expression has been thought to act as an immunomodulator molecule for anti-tumor immune response. The Hsp70 molecules secreted into the tumor microenvironment, would be taken up by DCs to activate the DCs for T cell-mediated immune response. Phagocytosed Hsp70 will be processed and presented on MHC-I and MHC-II complexes for T cells presentation. These caused DCs to express a high level of MHC-I and MHC-II as well as co-stimulatory molecules, CD80 and CD86 for effective T cells activation which was observed in this study. DC maturation is speculated to be mediated by upregulating IL-6 [46] and CCR-7 to mediate matured DC migration to LNs [40]. Due to the high population of matured DCs in the LNs, the treatment has been proposed to elevate the activation of T cells including cytotoxic $CD8^+$ and helper $CD4^+$ T in LNs. This has caused a high frequency of activated T cells to migrate out of lymph nodes and infiltrate into the tumor microenvironment which was observed in the current study. Anti-tumor immune response by T cells is suggested to be induced by upregulating TNF-α [47]. At the same time, it was observed that a combination of ox-MWCNTs and HT treatment downregulated the Tregs population. The elevated temperature might reduce the

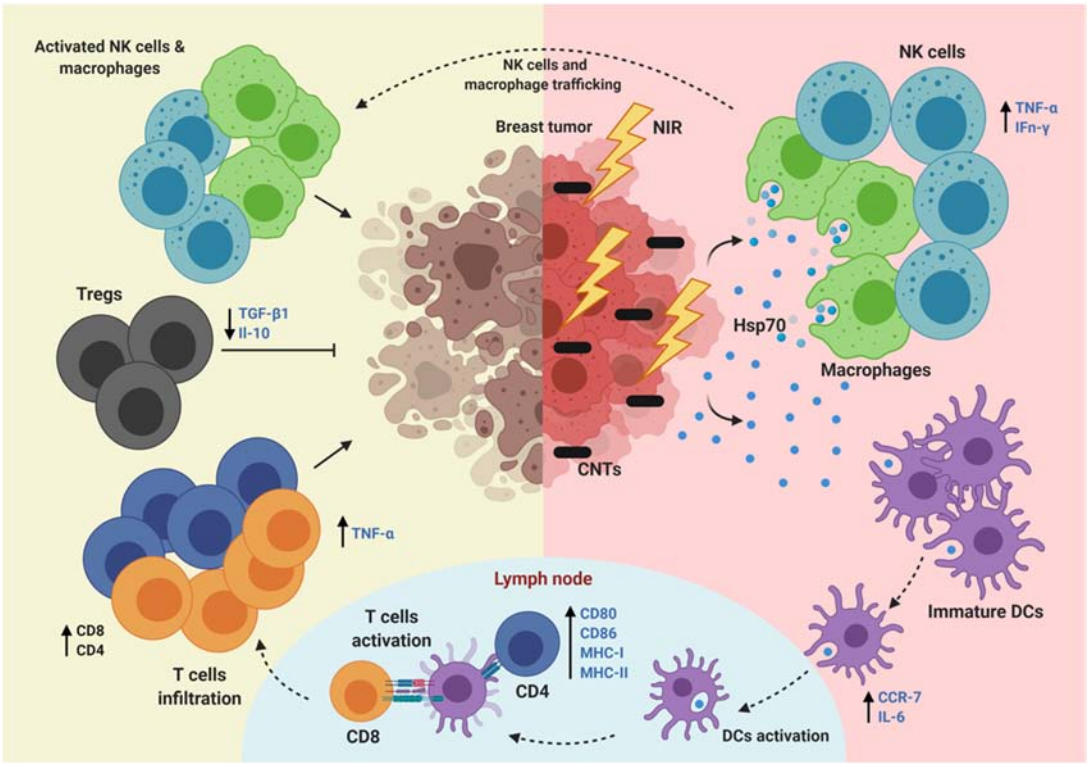

Fig. 7. Proposed mechanism of anti-tumor immune response inside tumor microenvironment following treatment with ox-MWCNTs and HT.

expression of immunosuppressive factors such as TGF-β1 and IL-10 [48], and thus inhibit infiltration and immunosuppressive ability of Tregs in the tumor microenvironment [49]. The increased expression of Hsp70 following combined treatment may also influence NK cells trafficking into the tumor microenvironment. Subsequently, the increase of NK cells trafficking in the tumor microenvironment contributes to enhance tumor killing actions. It has been reported that NK cells secreted TNF-α and IFN-γ [50] in which these cytokines are crucial for the recruitment of macrophage and tumor lysis [51]. In addition, Hsp70 can also promote macrophage recognition and recruitment into the tumor microenvironment. It is suggested that macrophages might promote anti-tumor response by secreting TNF-α in the tumor microenvironment [52]. Compared to other groups, both NK cells and macrophages were revealed to be found in larger populations after combined treatment. The simultaneous increased in both populations demonstrated enhanced tumor-killing activity induced by combined treatment. Furthermore, it is further speculated that anti-tumor immune responses were also affected by other immune mediators such as cytokines which would be worth to be explored in understanding the immunological effects of combined treatment on the tumor microenvironment. Altogether, both DCs maturation and immune cells infiltration were involved for the synergetic effect of ox-MWCNTs and HT in EMT6 cells, as observed in the present study.

5. Conclusion

In summary, our study has demonstrated the potential use of ox-MWCNTs as an effective hyperthermic agent in mediating local HT treatment for breast cancer. Our data suggest that a combination treatment of ox-MWCNTs and HT are able to eradicate EMT6 breast tumor and promote the infiltration of immune cells within the tumor microenvironment. Therefore, information from this study may provide a better understanding on the immune responses following ox-MWCNTs and HT and highlight the potential of this treatment regime as a minimally invasive treatment for breast cancer.

CRediT authorship contribution statement

Muhammad Redza Mohd Radzi: Conceptualization, Methodology, Validation, Formal analysis, Investigation, Writing – original draft, Visualization. **Nur Amanina Johari**; Investigation, Writing – original draft. **Wan Fatin Amira Wan Mohd Zawawi**; Methodology, Writing – review & editing. **Nurriza Ab. Latiff**; Conceptualization. **Nik Ahmad Nizam Nik Malik**; Writing – review & editing. **Nurliyana Ahmad Zawawi**; Methodology, Writing – review & editing. **Asnida Abdul Wahab**; Conceptualization. **Maheza Irna Salim**; Conceptualization, Resources. **Khairunadwa Jemon**; Conceptualization, Validation, Writing – review & editing, Supervision, Project administration, Funding acquisition.

Declaration of competing interest

The authors declare that they have no known competing financial interests or personal relationships that could have appeared to influence the work reported in this paper.

Acknowledgment

This study was funded by the Ministry of Higher Education, Malaysia (ref: FRGS/1/2015/SKK11/UTM/02/1 and FRGS/1/2018/SKK08/UTM/02/1) and Universiti Teknologi Malaysia (Q.J130000.2654.15J87). The authors thanked the Faculty of Science, Universiti Teknologi Malaysia for providing full support, access and facilities especially the Cancer Research Laboratory research group until this study was completed.

References

[1] F. Bray, et al., Global Cancer Statistics 2018: GLOBOCAN estimates of incidence and mortality worldwide for 36 cancers in 185 countries, CA Cancer J. Clin. 68 (6) (2018) 394–424.
[2] L. Tharmarajah, Complementary and alternative therapies for breast cancer worldwide, Lett. Health Biol. Sci. 3 (2) (2018) 27–32.

[3] A.R. Burke, et al., The resistance of breast cancer stem cells to conventional hyperthermia and their sensitivity to nanoparticle-mediated photothermal therapy, Biomaterials 33 (10) (2012) 2961–2970.
[4] S.-R. Ji, et al., Carbon nanotubes in cancer diagnosis and therapy, Biochim. Biophys. Acta Rev.Cancer 1806 (1) (2010) 29–35.
[5] H.K. Moon, S.H. Lee, H.C. Choi, In vivo near-infrared mediated tumor destruction by photothermal effect of carbon nanotubes, ACS Nano 3 (11) (2009) 3707–3713.
[6] J.R. Ostberg, et al., Regulatory potential of fever-range whole body hyperthermia on langerhans cells and lymphocytes in an antigen-dependent cellular immune response, J. Immunol. 167 (5) (2001) 2666–2670.
[7] T. Kikumori, et al., Anti-cancer effect of hyperthermia on breast cancer by magnetite nanoparticle-loaded anti-HER2 immunoliposomes, Breast Cancer Res. Treat. 113 (3) (2009) 435.
[8] N. Kawai, et al., Anticancer effect of hyperthermia on prostate cancer mediated by magnetite cationic liposomes and immune-response induction in transplanted syngeneic rats, Prostate 64 (4) (2005) 373–381.
[9] S. Toraya-Brown, S. Fiering, Local tumour hyperthermia as immunotherapy for metastatic cancer, Int. J. Hyperth. 30 (8) (2014) 531–539.
[10] J. Stauffer, M. Paulides, Hyperthermia therapy for cancer, 2014.
[11] W. Yin, et al., High-throughput synthesis of single-layer MoS2 nanosheets as a near-infrared photothermal-triggered drug delivery for effective cancer therapy, ACS Nano 8 (7) (2014) 6922–6933.
[12] Z. Zhang, J. Wang, C. Chen, Near-infrared light-mediated nanoplatforms for cancer thermo-chemotherapy and optical imaging, Adv. Mater. 25 (28) (2013) 3869–3880.
[13] N. Datta, et al., Local hyperthermia combined with radiotherapy and-/or chemotherapy: recent advances and promises for the future, Cancer Treat. Rev. 41 (9) (2015) 742–753.
[14] W.F.A.W.M. Zawawi, et al., Hyperthermia by near infrared radiation induced immune cells activation and infiltration in breast tumor, Sci. Rep. 11 (1) (2021) 1–13.
[15] P. Wust, et al., Hyperthermia in combined treatment of cancer, Lancet Oncol. 3 (8) (2002) 487–497.
[16] C.J. Gannon, et al., Carbon nanotube-enhanced thermal destruction of cancer cells in a noninvasive radiofrequency field, Cancer 110 (12) (2007) 2654–2665.
[17] N. Jafaripour, et al., Synthesize and characterization of a novel cadmium selenide nanoparticle with iron precursor applicable in hyperthermia of cancer cells, Int. J. Nanosci. Nanotechnol. 17 (2) (2021) 77–90.
[18] A. Najafinezhad, et al., Hydroxyapatite-M-type strontium hexaferrite: a new composite for hyperthermia applications, J. Alloys Compd. 734 (2018) 290–300.
[19] M.M. Salmani, et al., Synergic effects of magnetic nanoparticles on hyperthermia-based therapy and controlled drug delivery for bone substitute application, J. Supercond. Nov. Magn. 33 (2020) 2809–2820.
[20] A. Burke, et al., Long-term survival following a single treatment of kidney tumors with multiwalled carbon nanotubes and near-infrared radiation, Proc. Natl. Acad. Sci. 106 (31) (2009) 12897–12902 (p. pnas. 0905195106).
[21] J. Silvestre, N. Silvestre, J. De Brito, Review on concrete nanotechnology, Eur. J. Environ. Civ. Eng. 20 (4) (2016) 455–485.
[22] J. Lee, et al., Gold nanoparticles in breast cancer treatment: promise and potential pitfalls, Cancer Lett. 347 (1) (2014) 46–53.
[23] C. Wang, et al., Immunological responses triggered by photothermal therapy with carbon nanotubes in combination with anti-CTLA-4 therapy to inhibit cancer metastasis, Adv. Mater. 26 (48) (2014) 8154–8162.
[24] A. Jolesch, et al., Hsp70, a messenger from hyperthermia for the immune system, Eur. J. Cell Biol. 91 (1) (2012) 48–52.
[25] G. Multhoff, et al., The role of heat shock protein 70 (Hsp70) in radiation-induced immunomodulation, Cancer Lett. 368 (2) (2015) 179–184.
[26] B.R. Cassileth, G. Deng, Complementary and alternative therapies for cancer, Oncologist 9 (1) (2004) 80–89.
[27] R. Singh, S.V. Torti, Carbon nanotubes in hyperthermia therapy, Adv. Drug Deliv. Rev. 65 (15) (2013) 2045–2060.
[28] C.L. Ursini, et al., Study of cytotoxic and genotoxic effects of hydroxyl-functionalized multiwalled carbon nanotubes on human pulmonary cells, J. Nanomater. 2012 (2012) 7.
[29] N. Kobayashi, H. Izumi, Y. Morimoto, Review of toxicity studies of carbon nanotubes, J. Occup. Health 59 (5) (2017) 394–407 (p. 17–0089-RA).
[30] N.A. Zawawi, et al., Effect of acid oxidation methods on multiwalled carbon nanotubes (MWCNT) for drug delivery application, Int. J. Adv. Sci. Res. Manag. 1 (11) (2016) 14–22.
[31] J.T. Robinson, et al., High performance in vivo near-IR (> 1 μm) imaging and photothermal cancer therapy with carbon nanotubes, Nano Res. 3 (11) (2010) 779–793.
[32] A. Osorio, et al., H2SO4/HNO3/HCl—functionalization and its effect on dispersion of carbon nanotubes in aqueous media, Appl. Surf. Sci. 255 (5) (2008) 2485–2489.
[33] S. Wang, S.P. Jiang, X. Wang, Polyelectrolyte functionalized carbon nanotubes as a support for noble metal electrocatalysts and their activity for methanol oxidation, Nanotechnology 19 (26) (2008), 265601.
[34] N.A. Buang, et al., Characteristic of mild acid functionalized multiwalled carbon nanotubes towards high dispersion with low structural defects, Dig. J. Nanomater. Biostruct. 7 (1) (2012) 33–39.
[35] Z. Sobhani, et al., Photothermal therapy of melanoma tumor using multiwalled carbon nanotubes, Int. J. Nanomedicine 12 (2017) 4509.
[36] J. Kathi, K.-Y. Rhee, J.H. Lee, Effect of chemical functionalization of multi-walled carbon nanotubes with 3-aminopropyltriethoxysilane on mechanical and morphological properties of epoxy nanocomposites, Compos. A: Appl. Sci. Manuf. 40 (6–7) (2009) 800–809.
[37] M. Ibrahim, Functionalized Multiwalled Carbon Nanotubes for Salicylic Acid And Pseudoephiderine Drug Carrier System. Universiti Teknologi Malaysia, UTM, 2010 (Thesis, Master of Science (Chemistry)).
[38] J.W. Fisher, et al., Photothermal response of human and murine cancer cells to multiwalled carbon nanotubes after laser irradiation, Cancer Res. 70 (23) (2010) 9855–9864.
[39] P. Srivastava, Heat shock proteins in immune response to cancer: the fourth paradigm, Experientia 50 (11–12) (1994) 1054–1060.
[40] X. Wang, et al., MWCNT-mediated combinatorial photothermal ablation and chemo-immunotherapy strategy for the treatment of melanoma, J. Mater. Chem. B 8 (19) (2020) 4245–4258.
[41] S. Somersan, et al., Primary tumor tissue lysates are enriched in heat shock proteins and induce the maturation of human dendritic cells, J. Immunol. 167 (9) (2001) 4844–4852.
[42] G. Wang, et al., Magnetic fluid hyperthermia inhibits the growth of breast carcinoma and downregulates vascular endothelial growth factor expression, Oncol. Lett. 7 (5) (2014) 1370–1374.
[43] E.J. Comparetti, V.d.A. Pedrosa, R. Kaneno, Carbon nanotube as a tool for fighting cancer, Bioconjug. Chem. 29 (3) (2017) 709–718.
[44] X. Hou, et al., Nanoparticle-based photothermal and photodynamic immunotherapy for tumor treatment, Int. J. Cancer 143 (12) (2018) 3050–3060.
[45] C. Liu, et al., Treg cells promote the SREBP1-dependent metabolic fitness of tumor-promoting macrophages via repression of CD8 + T cell-derived interferon-γ, Immunity 51 (2) (2019) 381–397.e6.
[46] S. Lee, et al., Immunogenic effect of hyperthermia on enhancing radiotherapeutic efficacy, Int. J. Mol. Sci. 19 (9) (2018) 2795.
[47] H. Huang, et al., It's getting hot in here: targeting cancer stem-like cells with hyperthermia, J. Stem Cell Transplant. Biol. 2 (2) (2017).
[48] W. Ou, et al., Combination of NIR therapy and regulatory T cell modulation using layer-by-layer hybrid nanoparticles for effective cancer photoimmunotherapy, Theranostics 8 (17) (2018) 4574.
[49] J. Hu, et al., Response of regulatory T cells to classic heat stroke in mice, Exp. Ther. Med. 16 (6) (2018) 4609–4615.
[50] J. Domagala, et al., The tumor microenvironment—a metabolic obstacle to NK cells' activity, Cancers 12 (12) (2020) 3542.
[51] S.S. Evans, E.A. Repasky, D.T. Fisher, Fever and the thermal regulation of immunity: the immune system feels the heat, Nat. Rev. Immunol. 15 (6) (2015) 335–349.
[52] E.Y. Komarova, et al., Extracellular Hsp70 reduces the pro-tumor capacity of monocytes/macrophages co-cultivated with cancer cells, Int. J. Mol. Sci. 21 (1) (2020) 59.